

# Remote Phenology: Applying Machine Learning to Detect Phenological Patterns in a Cerrado Savanna

Jurandy Almeida<sup>1</sup>, Jefersson A. dos Santos<sup>1</sup>, Bruna Alberton<sup>2</sup>,  
Ricardo da S. Torres<sup>1</sup>, and Leonor Patricia C. Morellato<sup>2</sup>

<sup>1</sup> RECOD Lab, Institute of Computing, University of Campinas – UNICAMP  
13083-852, Campinas, SP – Brazil  
Email: {jurandy.almeida, jsantos, rtorres}@ic.unicamp.br

<sup>2</sup> Phenology Lab, Dept. of Botany, Sao Paulo State University – UNESP  
13506-900, Rio Claro, SP – Brazil  
Email: bru.alberton@gmail.com, pmorella@rc.unesp.br

**Abstract**—Plant phenology has gained importance in the context of global change research, stimulating the development of new technologies for phenological observation. Digital cameras have been successfully used as multi-channel imaging sensors, providing measures of leaf color change information (RGB channels), or leafing phenological changes in plants. We monitored leaf-changing patterns of a cerrado-savanna vegetation by taken daily digital images. We extract RGB channels from digital images and correlated with phenological changes. Our first goals were: (1) to test if the color change information is able to characterize the phenological pattern of a group of species; and (2) to test if individuals from the same functional group may be automatically identified using digital images. In this paper, we present a machine learning approach to detect phenological patterns in the digital images. Our preliminary results indicate that: (1) extreme hours (morning and afternoon) are the best for identifying plant species; and (2) different plant species present a different behavior with respect to the color change information. Based on those results, we suggest that individuals from the same functional group might be identified using digital images, and introduce a new tool to help phenology experts in the species identification and location on-the-ground.

## I. INTRODUCTION

Phenology, the study of natural recurring phenomena and its relation to climate [1], is a traditional science dedicated to the observation of the cycles of plants and animals and relate mainly to local meteorological data, as well as to biotic interactions and phylogeny [2].

The leaf flushing and senescence are important events in plants cycles and are fundamental to understand a range of processes in the ecosystem due to their impact on growth, water status, gas exchange, and nutrient cycling [3], [4]. The plants growing season plays a crucial role on the carbon balance and in the terrestrial productivity [5]–[7], and controls spatial and temporal patterns of C and water exchange between forest and atmosphere [8], [9].

Plant phenology has gained importance as the simplest and most reliable indicator in the context of global change research, stimulating the development of new technologies for phenological observation [10]–[14]. Digital cameras have been

successfully used as multi-channel imaging sensors, and the measurements of color change information (RGB channels) from digital images allow to detect phenological changes events in plants [14]–[19].

After quantifying the color channels, it is possible to estimate changes on phenological events, such as leaf flushing when analyzing the green channel, or leaf color change and senescence using values from the red channel [14], [16]. However, image information from digital camera are sparse for high diverse tropical forest, where one image may encompass dozens to more than a hundred species, compared to the low number of species on temperate vegetations.

We monitored a tropical cerrado savanna vegetation to accesses the reliability of digital images to detect leaf changes and validate the digital data with on the ground direct phenological observation. Our first experiments are intended to respond the following research questions:

- 1) Is the color change information able to characterize the phenological pattern of a group of species?
- 2) Is it possible to automatically identify individuals of the same functional group using digital images?

## II. MULTI-SCALE CLASSIFIER

The *multi-scale classifier* (MSC) [20] is a learning strategy based on boosting of weak learners [21]. It aims at assigning a label (+1 for relevant class, and −1 otherwise) to each pixel  $p$  of  $P_0$  taking advantage of various features computed on regions of various levels from a segmentation hierarchy. The final classifier is a linear combination  $MSC(p)$  of  $T$  weak classifiers  $h_t(p)$ :

$$MSC(p) = \text{sign}\left(\sum_{t=1}^T \alpha_t h_t(p)\right), \quad (1)$$

where  $\alpha_t$  is the weight assigned to the weak classifier  $h_t(p)$  at the iteration  $t$ .

The MSC training repeatedly calls *weak learners* in a series of rounds  $t = 1, \dots, T$ . Each weak learner creates a weak

classifier that decreases the expected classification error of the combination. The algorithm then selects the weak classifier that most decreases the error.

The strategy consists in keeping a set of weights over the training set. These weights can be interpreted as a measure of the difficulty level to classify each training sample. At the beginning, all the pixels have the same weight, but in each round, the weights of the misclassified pixels are increased. Thus, in the next rounds the weak learners are forced to focus on harder samples. We will note  $W_t(p)$  the weight of pixel  $p$  in round  $t$ , and  $D_{t,\lambda}(R)$  the misclassification rate of region  $R$  in round  $t$  at scale  $\lambda$  given by the mean of the weights of its pixels:

$$D_{t,\lambda}(R) = \left( \frac{1}{|R|} \sum_{p \in R} W_t(p) \right). \quad (2)$$

Algorithm 1 presents the training process of our MSC. Let  $Y_\lambda(R)$ , the set of labels of regions  $R$  at scale  $\lambda$ , be the training set. In a series of rounds  $t = 1, \dots, T$ , for all scales  $\lambda$ , the weight of each region  $D_{t,\lambda}(R)$  is computed (line 3). This piece of information is used to select the regions to be used for training the weak learners, building a subset of labeled regions  $\hat{Y}_{t,\lambda}$  (line 6). The subset  $\hat{Y}_{t,\lambda}$  is used to train the weak learners with each features  $\mathcal{F}$  at scale  $\lambda$  (line 9). Each weak learner produces a weak classifier  $h_{t,(\mathcal{F},\lambda)}$  (line 10). The algorithm then selects the weak classifier  $h_t$  that most decreases the error  $Err_{h_t}$  (line 12). The level of error of  $h_t$  is used to compute the coefficient  $\alpha_t$ , which indicates the degree of importance of  $h_t$  in the final classifier (line 13). The selected weak classifier  $h_t$  and the coefficient  $\alpha_t$  are used to update the weights of the pixels  $W_{(t+1)}(p)$  which can be used in the next round (line 14).

The classification error of the classifier  $h$  is:

$$Err(h, W) = \sum_{p|h(p)Y_0(p) < 0} W(p). \quad (3)$$

The training is performed on the training set labels  $Y_\lambda$  corresponding to the same scale  $\lambda$ . The weak learners (linear SVM, for example) use the subset  $\hat{Y}_{t,\lambda}$  for training and produce a weak classifier  $h_{t,(\mathcal{F},\lambda)}$ . The training set labels  $Y_0$  are the labels of pixels of image  $I$ , and training sets labels  $Y_\lambda$  with  $\lambda > 0$  are defined according to the proportions of pixels belonging to one of the two classes (for example, at least 80% of one region).

#### A. SVM-based weak learner

In this work, we used a linear SVM (support vector machine) as weak learner, which is an SVM trainer based on a specific feature type  $\mathcal{F}$  and a specific scale  $\lambda$ . Given the training subset labels  $\hat{Y}_\lambda$ , the strategy is to find the best linear hyperplane of separation between the regions according to their classes, trying to maximize the data separation margin. These samples are called support vectors and are found during the training. Once the support vectors and the decision coefficients ( $\alpha_i, i = 1, \dots, N$ ) are found, the SVM weak classifier

---

### Algorithm 1 Multi-Scale Classifier

---

Given:

Training labels  $Y_\lambda(R)$  = labels of regions  $R$  at scale  $\lambda$

Initialize:

For all pixels  $p$ ,  $W_1(p) \leftarrow \frac{1}{|Y_0|}$ , where  $|Y_0|$  is the number of pixels in the image level

```

1 For  $t \leftarrow 1$  to  $T$  do
2   For all scales  $\lambda$  do
3     For all  $R \in P_\lambda$  do
4       Compute  $D_{t,\lambda}(R)$ 
5     End for
6     Build  $\hat{Y}_{t,\lambda}$  (a training subset based on  $D_{t,\lambda}(R)$ )
7   End for
8   For each pair feature/scale  $(\mathcal{F}, \lambda)$  do
9     Train weak learners using features  $(\mathcal{F}, \lambda)$  and
    training set  $\hat{Y}_{t,\lambda}$ .
10    Evaluate resulting classifier  $h_{t,(\mathcal{F},\lambda)}$ : compute
     $Err(h_{t,(\mathcal{F},\lambda)}, W)$  (Equation 3)
11  End for
12  Select weak classifier
     $h_t = \operatorname{argmin}_{h_{t,(\mathcal{F},\lambda)}} Err(h_{t,(\mathcal{F},\lambda)}, W_{t,\lambda})$ 
13  Compute  $\alpha_t \leftarrow \frac{1}{2} \ln \left( \frac{1+r_t}{1-r_t} \right)$  with  $r_t \leftarrow \sum_p cY_0(p)h_t(p)$ 
14  Update  $W_{t+1}(p) \leftarrow \frac{W_t(p) \exp(-\alpha_t Y_0(p)h_t(p))}{\sum_p W_t(p) \exp(-\alpha_t Y_0(p)h_t(p))}$ 
15 End for

```

Output: Multi-Scale Classifier  $MSC(p)$

---

can be defined as:

$$SVM_{(\mathcal{F},\lambda)}(R) = \operatorname{sign} \left( \sum_i^N y_i \alpha_i (f_R \cdot f_i) + b \right), \quad (4)$$

where  $b$  is a parameter found during the training. The support vectors are the  $f_i$  such that  $\alpha_i > 0$ ,  $y_i$  is the support vector class and  $f_R$  is the feature vector of the region.

The training subset  $\hat{Y}_{t,\lambda}$  is composed by  $n$  labels from  $Y_\lambda$  with values of  $D_{t,\lambda}(R)$  larger or equal to  $\frac{1}{|Y_0|}$ . This strategy means that only regions considered as the most difficult ones are used for the training. For the first round of boosting, the regions to compose the subset  $\hat{Y}_{0,\lambda}$  are randomly selected.

## III. MATERIALS AND METHODS

### A. Study Area and Camera Setup

The near remote phenological system was set up in a 18m tower in a Cerrado sensu stricto, a savanna-like vegetation located at Itirapina (22°10'49.18"S / 47°52'16.54"O), São Paulo State, Brazil. The cerrado stricto sensu is a savanna-like vegetation presenting a discontinuous canopy and woody component reaching six to seven meters high and a continuous

herbaceous layer. In some parts, the vegetation is denser, with some trees reaching up to 12m high. The cerrado savanna study site is about 260ha, 610m altitude and the regional climate is Cwa type according to Köppen classification. The average climate (1972 to 2002) shows a mean annual total rainfall of 1524mm and mean temperature of 20.7°C, with one warm, humid season from October to March (average of 22°C and 78% of annual precipitation) and one cool, dry season from April to September (average of 18°C and 16% of annual precipitation).

A digital hemispherical lens camera (Mobotix Q24) was setup at the top of the phenology tower, attached in an iron arm facing northeast (Figure 1). The camera activity is controlled by a timer and the energy source is a 12V battery charged by a solar panel. We installed also a complete climate station (Data Logger U30 GSM) on 1st December for the collection of microclimatic data, with remote access using 3G internet.



Fig. 1. The cerrado-savanna phenology tower (18m tall), where the digital hemispherical lens camera was set up (red arrow) attached in an iron arm facing northeast.

The first data collection from the digital camera started on 18th August 2011. We set up the camera to automatically take a daily sequence of five JPEG images (at 1280 × 960 pixels of resolution) per hour, from 6:00 to 18:00 hs. The present study was based on the analysis of over 2,700 images, recorded between August 28th and October 3rd, 2011 (Figure 2), during the main leafing season.

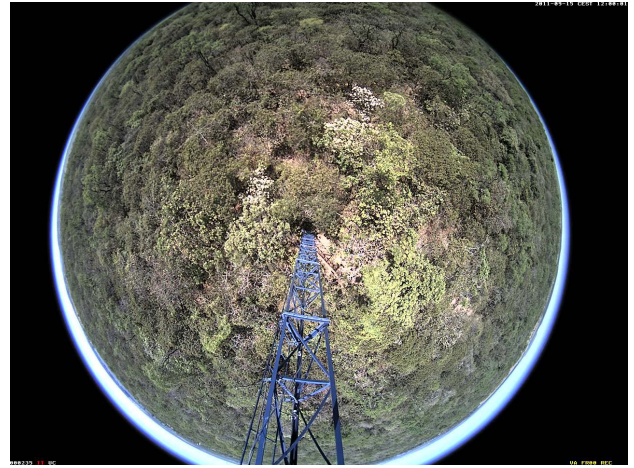


Fig. 2. Sample image of the cerrado savanna recorded by the digital camera on October 15th, 2011.

### B. Image Analysis

The image analysis was conducted by defining different regions of interest (ROI), as described by Richardson *et al.* [15], Richardson *et al.* [14], and Ahrends *et al.* [16]. For each ROI, a binary image with the same dimensions of the original image was created as a mask. White pixels of a mask indicate the ROI, while the remaining area was filled by black pixels. We defined six ROIs (Figure 3) based on the random selection of six plant species identified in the hemispheric image: (1) *Aspidosperma tomentosum* (Figure 3(a)), (2) *Caryocarp brasiliensis* (Figure 3(b)), (3) *Myrcia guianensis* (Figure 3(c)), (4) *Miconia rubiginosa* (Figure 3(d)), (5) *Pouteria ramiflora* (Figure 3(e)), and (6) *Pouteria torta* (Figure 3(f)).

We analyzed each ROI in the terms of the contribution of the primary colors (Red, Green, and Blue), as proposed by Richardson *et al.* [15]. Initially, a custom script was used to analyze each color channel and to compute the average value of the pixel intensity. After that, we calculated the relative (or normalized) brightness of each color channel, as:

$$\begin{aligned} Total_{avg.} &= Red_{avg.} + Green_{avg.} + Blue_{avg.} \quad (5) \\ \% \text{ of Red} &= \frac{Red_{avg.}}{Total_{avg.}} \\ \% \text{ of Green} &= \frac{Green_{avg.}}{Total_{avg.}} \\ \% \text{ of Blue} &= \frac{Blue_{avg.}}{Total_{avg.}} \end{aligned}$$

Figure 4 shows the behavior of those values for each ROI along the whole period, considering only the digital images taken at the midday. Each line corresponds to a time series for the variation of the normalized brightness of each color channel. Notice the differences between the behavior of each specie individually, reflecting the leaf color changes over the leaf life cycle or aging process.

According to the leaf exchange data from the on-the-ground field observations on leaf fall and leaf flush at our study site,

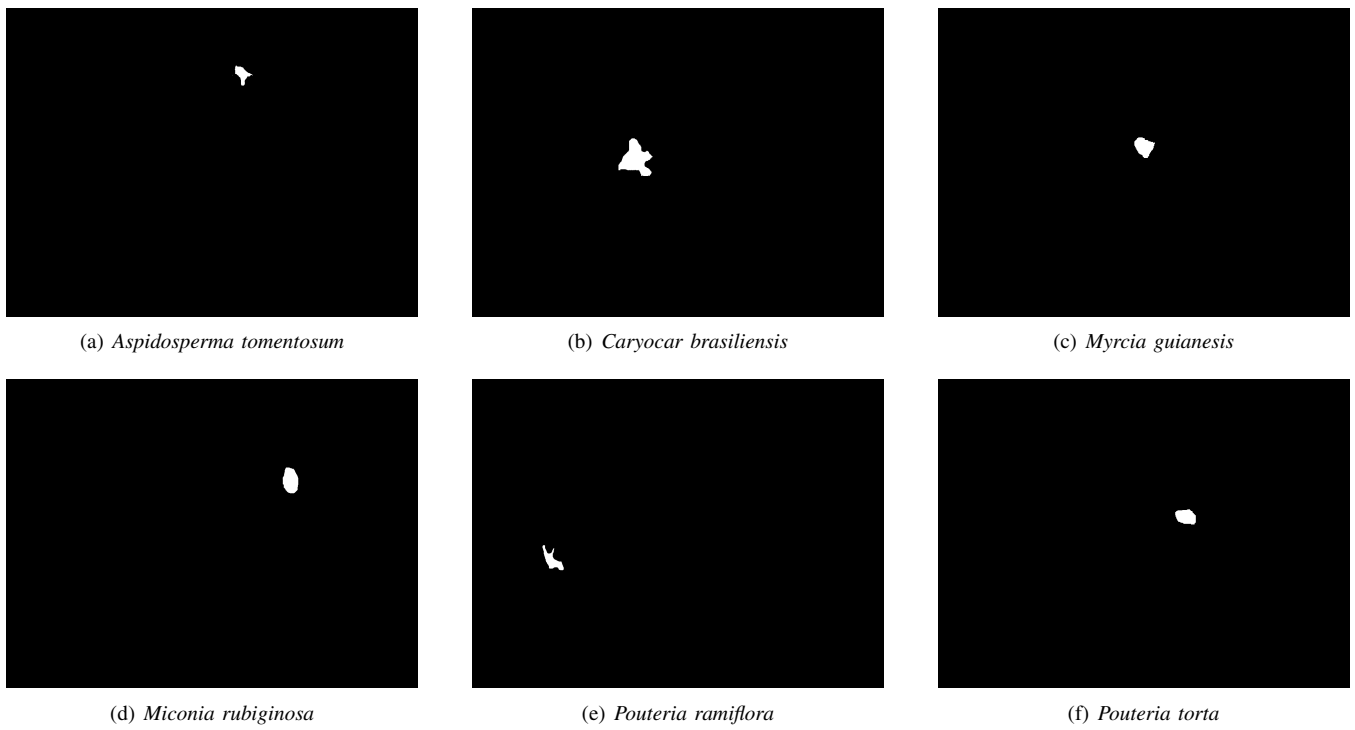


Fig. 3. Regions of interest (ROIs) defined for the analysis of cerrado-savanna digital images: (a) *Aspidosperma tomentosum*, (b) *Caryocar brasiliensis*, (c) *Myrcia guianensis*, (d) *Miconia rubiginosa*, (e) *Pouteria ramiflora*, and (f) *Pouteria torta*.

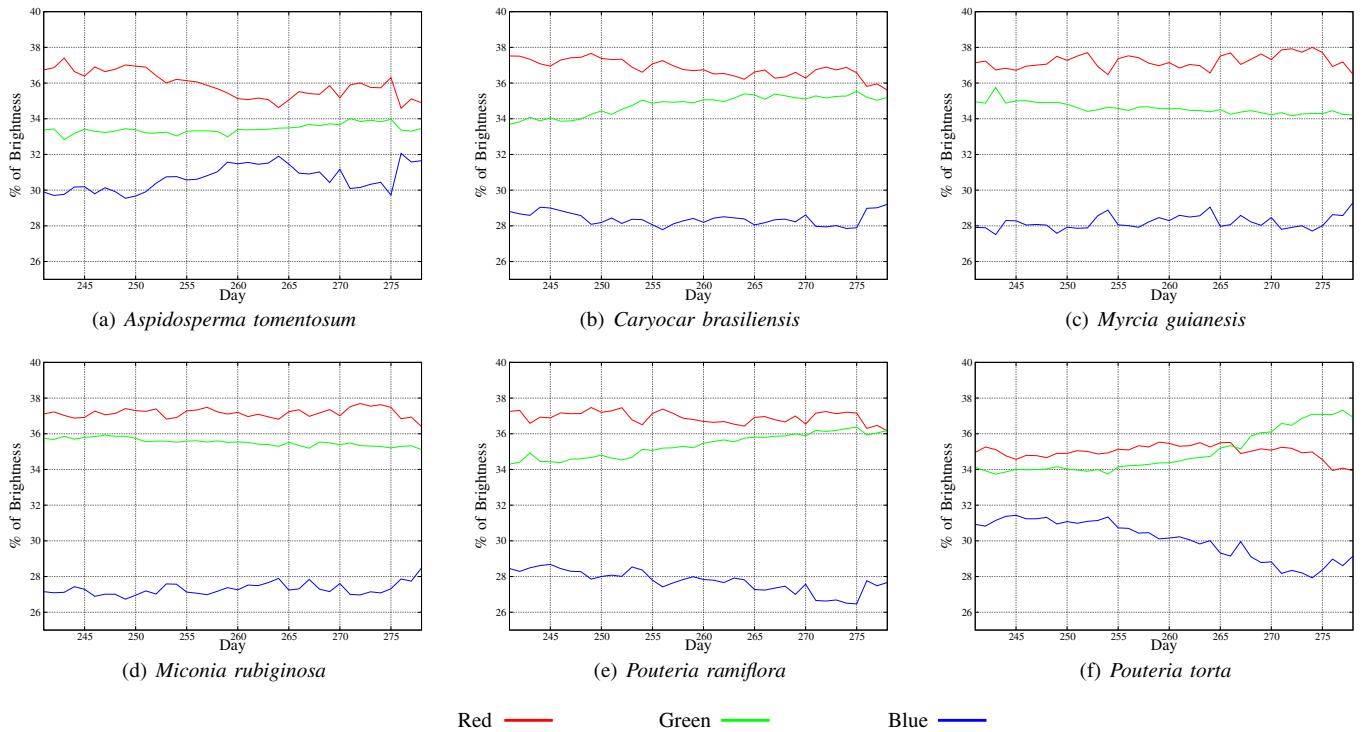


Fig. 4. The variance of the normalized brightness of each color channel from the digital images taken at the midday, each Julian day (August 28th to October 3rd, 2011), in the cerrado savanna using different regions of interest (ROIs), as described in Figure 3.

those species can be classified on three functional groups: (i) *Miconia rubiginosa*, *Pouteria ramiflora*, and *Pouteria torta*. deciduous, *Aspidosperma tomentosum* and *Caryocar brasiliensis*; (ii) evergreen, *Myrcia guianensis*; and (iii) semideciduous,

### C. Machine Learning

Figure 5 illustrates the steps of our MSC approach. The first step is to build a hierarchy of regions  $H$ . We have used Guigues algorithm [22] to perform the segmentation.

The image used to obtain the hierarchy of segmented regions was taken at noon on October 15th, 2011 (Figure 2). We have selected 5 segmentation scales from the hierarchy to perform feature extraction. The finest scale is composed by 27,380 regions and the coarsest scale contains 8,849 regions. Figure 6 illustrates the segmented scales in a subimage sample from Figure 2.

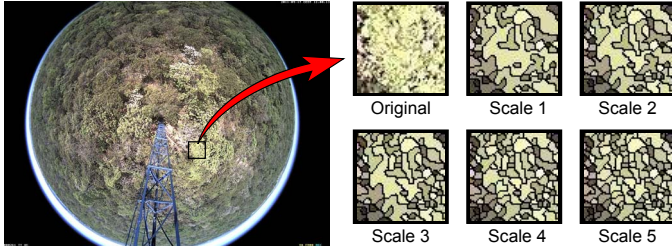


Fig. 6. The segmentation results for the selected scales in a subimage sample.

The second step is the feature extraction, which is carried out on the regions at different segmentation scales. For each plant specie, we have tested 39 different features by considering the time series on the available periods during the day (13 hours: from 6:00 to 18:00 hs) and the color channels (3 bands: R, G, and B),

Finally, we use the MSC (Algorithm 1) to build a linear combination of weak classifiers, each of them related to a specific scale and feature. This step was performed for each plant species by using their ROIs (Figure 3). To build a classifier for a given specie, we used the regions from its corresponding ROI as positive samples and from ROIs of the other species as negative samples. At the end, the final classifier was applied to classify the remaining regions of the image.

## IV. RESULTS AND PRELIMINARY DISCUSSION

### A. Classification Accuracy

We carried out experiments to classify the plant species in the image. For that, we selected two species from different functional groups: *Aspidosperma tomentosum* and *Miconia rubiginosa*. Next, we built a classifier for each specie using the approach described in Section III-C.

Figure 7 shows the ROIs used to build and analyze each of the classifiers. In this figure, green areas indicate individuals of the analyzed species, whose regions obtained from the segmentation were used as positive samples; while red areas represent individuals from other species, whose the segmented regions were considered as negative samples.

To assess the effectiveness of each classifier, two other individuals (yellow areas) from each of the analyzed species were chosen as a validation set. Then, we used the segmented regions extracted from those ROIs as input samples for each

of the classifiers. Thus, we can measure the classification accuracy as the ratio of the number of samples correctly classified as belonging to the analyzed species to the total number of samples in the validation set.

Figure 8 shows the classification accuracy for each of the color channels (3 bands: R, G, and B) along all the available periods of the day (13 hours: from 6:00 to 18:00 hs), totaling 39 different features for each of the analyzed species.

Figure 9 shows a different view of those results, including all the feature combinations, totaling 56 different possibilities. They are: (i) 1 hour of the day and 1 color channel (39 combinations); (ii) 1 hour of the day and all the color channels (13 combinations); (iii) all the hours of the day and 1 color channel (3 combinations); and (iv) all the hours of the day and all the color channels (1 combination). In order to make the comparison easier, we sorted the results from higher to lower accuracy.

Observe that, with less sunshine (early in the morning and late in the afternoon), the classification accuracy is higher, characterizing better the analyzed species for that particular day. It indicates that early and late hours are better to characterize the phenological pattern of plant species. Notice also the differences between the behavior of each specie individually with respect to the color channels, indicating different patterns of leaf color change.

As mentioned in Section II-A, the MSC approach is based on boosting weak learners. In this paper, each weak learner is a linear SVM classifier using features extracted from a given segmentation scale. In this way, each of the color channels along all the available periods of the day at one of the scales are used as a distinct feature. Table I presents the weak classifiers chosen by MSC training algorithm for the *Aspidosperma tomentosum* and *Miconia rubiginosa* species.

TABLE I  
WEAK CLASSIFIERS CHOSEN BY THE MSC FOR EACH ROUND  $t$ . THE CLASSIFIER IS COMPOSED BY: COLOR BAND, HOUR OF THE DAY AND SEGMENTATION SCALE.

$t$	Aspidosperma		Miconia rubiginosa	
	Classifier	Weight	Classifier	Weight
0	7h,R, $\lambda_5$	3.9	18h,R, $\lambda_2$	4.0
1	16h,B, $\lambda_4$	1.0	18h,R, $\lambda_3$	3.7
2	16h,B, $\lambda_2$	4.1	18h,R, $\lambda_5$	1.0
3	16h,R, $\lambda_5$	1.0	18h,R, $\lambda_5$	1.0
4	7h,B, $\lambda_2$	4.6	18h,R, $\lambda_5$	1.0
5	7h,B, $\lambda_5$	1.0	18h,R, $\lambda_5$	1.0
6	7h,B, $\lambda_4$	1.0	18h,R, $\lambda_5$	1.0
7	16h,B, $\lambda_4$	5.2	18h,R, $\lambda_5$	1.0
8	7h,B, $\lambda_4$	1.0	18h,R, $\lambda_5$	1.0
9	7h,B, $\lambda_5$	6.3	18h,R, $\lambda_5$	1.0

Those results confirm that the extreme hours (morning and afternoon) are better to characterize plant species. In addition, they also show that the *Aspidosperma tomentosum* and *Miconia rubiginosa* species present a different behavior with respect to the color channels. Moreover, it is interesting to note that fine scales provide better results than coarse ones for the species identification.

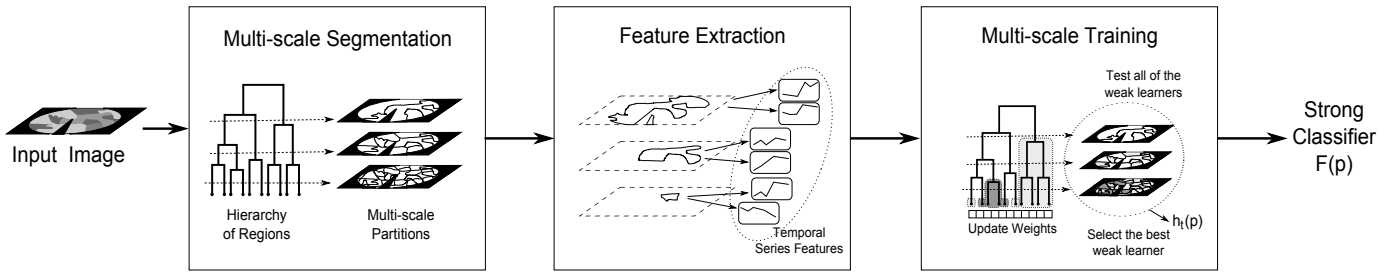


Fig. 5. Steps of the multi-scale learning process. Adapted from [20].

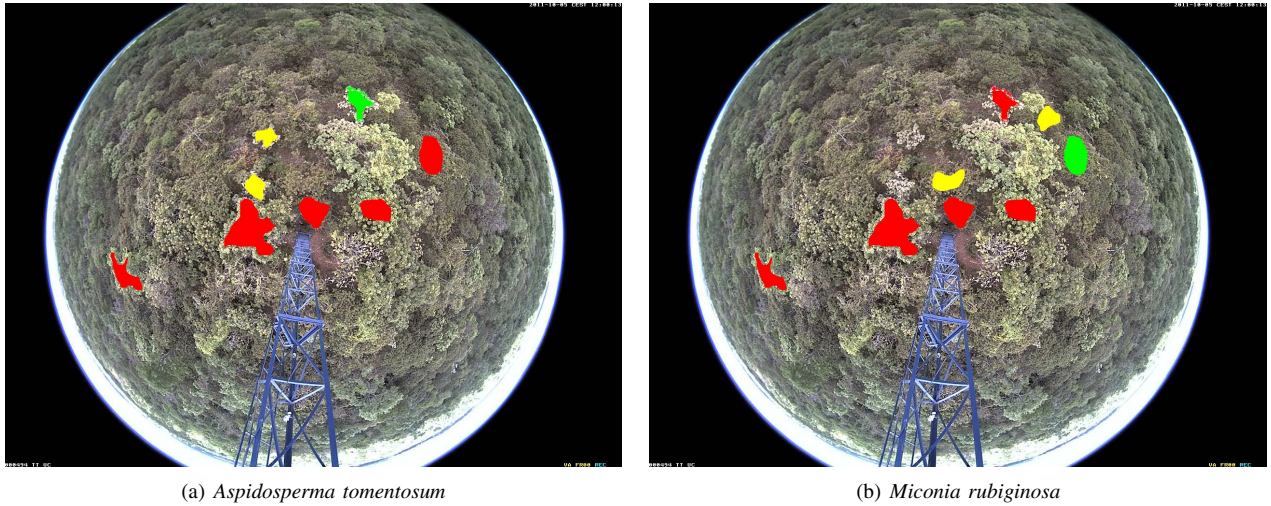


Fig. 7. Regions of interest (ROIs) used to build and analyze classifiers: green and red areas indicate individuals of plant species taken, respectively, as positive and negative samples for training; whereas yellow areas indicate individuals of plant species chosen for validation.

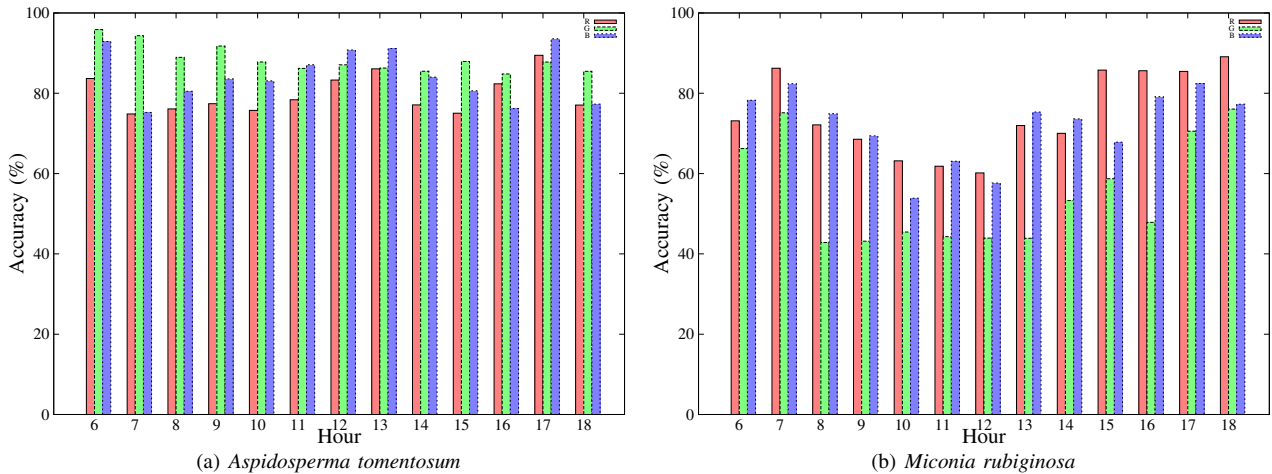


Fig. 8. Classification accuracy for each of the color channels along all the available periods of the day.

The main reason for those results is probably related to the leaf change pattern and species functional group, but may also be related to the specific leaf color of those species. These patterns indicate slightly different behavior for the analyzed species that need further in-depth analyses considering their on-the-ground phenology. Based on those results, our preliminary analysis suggests that individuals from the same functional group might be identified using digital images.

### B. Application in Phenology Studies

The species identification on-the-ground is very difficult since it requires an exhaustive analysis over a very large area. In this sense, our approach can help phenology experts to focus their analysis over a much smaller area, making such a task much easier and faster.

For that, we use the MSC approach to classify segmented regions from the digital images. Next, we create an image

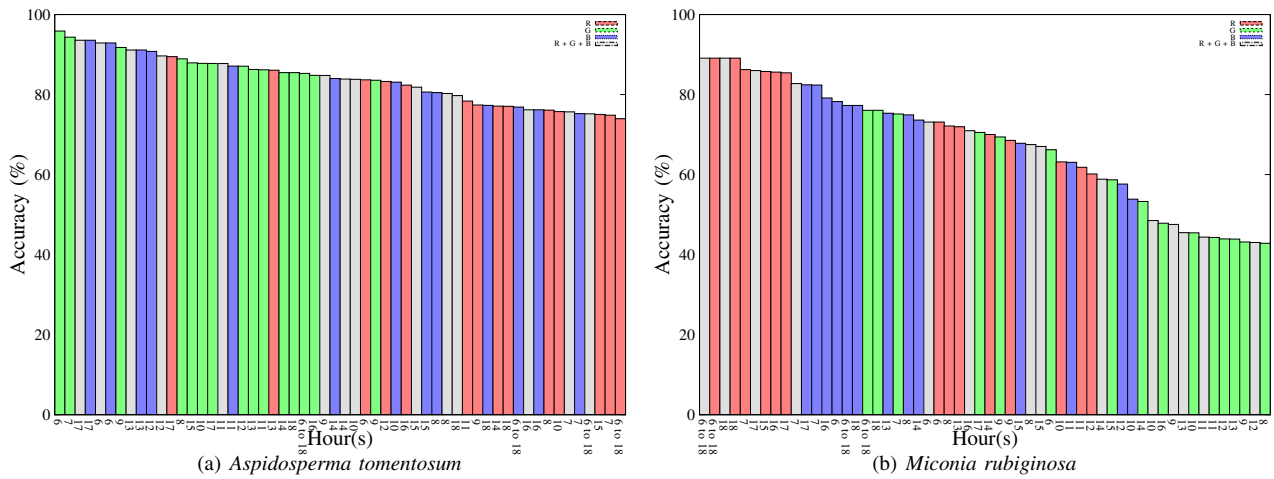


Fig. 9. The classification accuracies for each of the color channels along all the available periods of the day (among all the possible combinations).

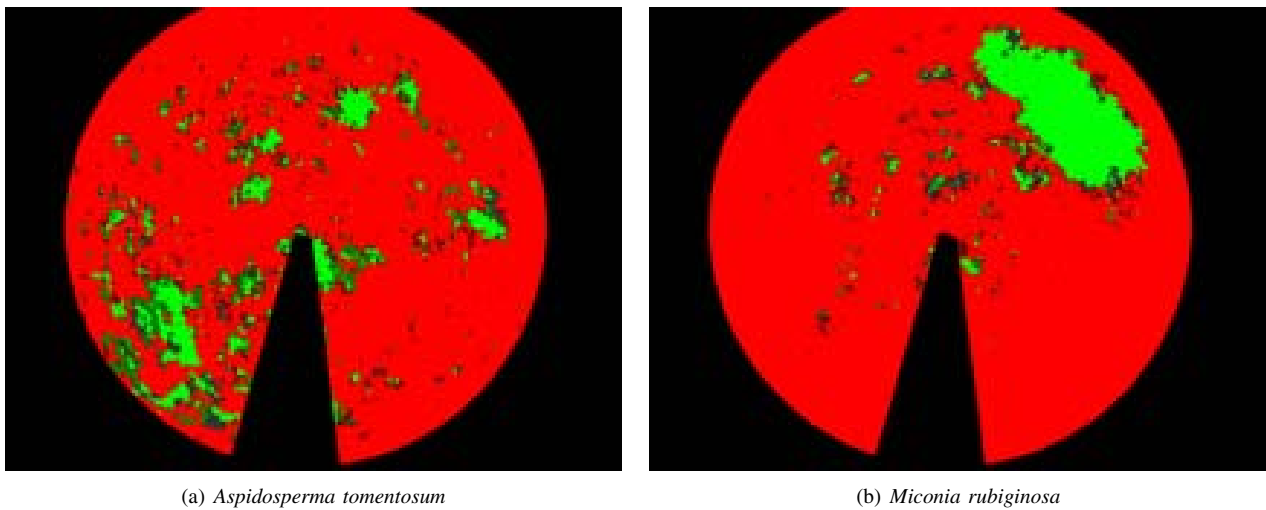


Fig. 10. Image maps produced for different species using the feature combination with the highest classification accuracy.

map based on the assigned labels, indicating graphically the areas where the probability of finding individuals from a given species is higher.

Figure 10 presents the image maps produced for the analyzed species using the feature combination that achieved the highest classification accuracy (i.e., 6h/G, for the *Aspidosperma tomentosum*; and 6-18h/RGB, for the *Miconia rubiginosa*). Different color scales were used to maximize the difference between the assigned labels: (i) a green scale, for similar patterns (between +1.0 and +0.3); (ii) a gray scale, for undefined patterns (between +0.3 and -0.3); and (iii) a red scale, for inverted patterns (between -0.3 and -1.0).

In this figure, the green areas indicate the segmented regions with a high probability of belonging to the same species. Notice how the study area can be greatly reduced by employing our approach. This opens up a number of possibilities that deserve much deeper study, but an immediate consequence is that we can help phenology experts with a new tool to identify plant species, increasing their accuracy on defining

the relationship between phenology and climate.

## V. PRELIMINARY CONCLUSIONS

We conclude that machine learning can be applied to detect phenological patterns in the high diversity of the tropical cerrado savanna vegetation. Using a conventional tool to measure the color change information, we were able to define the best hours of the day for characterizing plant species. The extreme hours (morning and afternoon) have shown the best results. Therefore, further studies do not need to cover all day long with digital images. Moreover, the data validation at species level have also revealed that different plant species present a different behavior with respect to the color change information. In this way, we were able to distinguish functional groups of plants using digital images. Finally, based on those results, we have introduced a new tool to help phenology experts in the species identification on-the-ground, making such a task much easier and faster.

#### ACKNOWLEDGMENT

This research was partially supported by Microsoft Research and Brazilian agencies FAPESP (grants 2007/52015-0, 2007/52015-0, 2009/18438-7, 2010/52113-5, and 2011/11171-5), CNPq (grant 306587/2009-2), and CAPES.

#### REFERENCES

- [1] M. D. Schwartz, *Phenology: An Integrative Environmental Science*. Academic Publishers, 2003.
- [2] B. Rathcke and E. P. Lacey, "Phenological patterns of terrestrial plants," *Annual Review of Ecology and Systematics*, vol. 16, pp. 179–214, 1985.
- [3] P. B. Reich, "Phenology of tropical forests: Patterns, causes and consequences," *Canadian Journal of Botany*, vol. 73, pp. 164–174, 1995.
- [4] G. C. S. Negi, "Leaf and bud demography and shoot growth in evergreen and deciduous trees of central himalaya, india," *Trees*, vol. 20, pp. 416–429, 2006.
- [5] C. D. Keeling, J. F. S. Chin, and T. P. Whorf, "Increased activity of northern vegetation inferred from atmospheric co2 measurements," *Nature*, vol. 382, pp. 146–149, 1996.
- [6] T. Rotzer, R. Grote, and H. Pretzsch, "The timing of bud burst and its effect on tree growth," *International Journal of Biometeorology*, vol. 48, pp. 109–118, 2004.
- [7] D. Loustau, A. Bosc, A. Colin, H. Davi, C. François, E. Dufrêne, M. Équé, E. Cloppet, D. Arrouays, C. Le Bas, N. Saby, G. Pignard, N. Hamza, A. Granier, N. Breda, P. Ciais, N. Viovy, J. Ogée, and J. Delage, "Modeling the climate change effects on the potential reduction of french plains forests at the sub regional level," *Tree Physiol*, vol. 25, pp. 813–823, 2005.
- [8] M. A. White, S. W. Running, and P. E. Thornton, "The impact of growing-season length variability on carbon assimilation and evapotranspiration over 88 years in the eastern us deciduous forest," *International Journal of Biometeorology*, vol. 42, pp. 139–145, 1999.
- [9] M. D. Schwartz, B. C. Reed, and M. A. White, "Assessing satellite derived start-of-season measures in the coterminous," *International Journal of Climatology*, vol. 22, pp. 1793–1805, 2002.
- [10] G. R. Walther, E. Post, P. Convey, A. Menzel, C. Parmesan, T. J. C. Beebee, J. M. Fromentin, O. Hoegh-Guldberg, and F. Bairlein, "Ecological responses to recent climate change," *Nature*, vol. 416, pp. 389–395, 2002.
- [11] C. Parmesan and G. A. Yohe, "A globally coherent fingerprint to climate change impacts accross natural systems," *Nature*, vol. 421, pp. 37–42, 2003.
- [12] G. R. Walther, "Plants in a warmer world," *Perspectives in Plant Ecology Evolution and Systematics*, vol. 6, pp. 169–185, 2004.
- [13] C. Rosenzweig, D. Karoly, M. Vicarelli, P. Neofotis, Q. Wu, G. Casassa, A. Menzel, T. L. Root, N. Estrella, B. Seguin, P. Tryjanowski, C. Liu, S. Rawlins, and A. Imeson, "Attributing physical and biological impacts to anthropogenic climate change," *Nature*, vol. 453, pp. 353–357, 2008.
- [14] A. D. Richardson, B. H. Braswell, D. Y. Hollinger, J. P. Jenkins, and S. V. Ollinger, "Near-surface remote sensing of spatial and temporal variation in canopy phenology," *Ecological Applications*, vol. 19, pp. 1417–1428, 2009.
- [15] A. D. Richardson, J. P. Jenkins, B. H. Braswell, D. Y. Hollinger, S. V. Ollinger, and M. L. Smith, "Use of digital webcam images to track spring greep-up in a deciduous broadleaf forest," *Oecologia*, vol. 152, pp. 323–334, 2007.
- [16] H. Ahrends, S. Etzold, W. Kutsch, R. Stoeckli, R. Bruegger, F. Jeanneret, H. Wanner, N. Buchmann, and W. Eugster, "Tree phenology and carbon dioxide fluxes: Use of digital photography for process-based interpretation at the ecosystem scale," *Climate Research*, vol. 39, pp. 261–274, 2009.
- [17] R. Ide and H. Oguma, "Use of digital cameras for phenological observations," *Ecological Informatics*, vol. 5, pp. 339–347, 2010.
- [18] S. Kurc and L. Benton, "Digital image-derived greenness links deep soil moisture to carbon uptake in a creosotebush-dominated shrubland," *Journal of Arid Environments*, vol. 74, pp. 585–594, 2010.
- [19] S. Nagai, T. Maeda, M. Gamo, H. Muraoka, R. Suzuki, and K. N. Nasahara, "Using digital camera images to detect canopy condition of deciduous broad-leaved trees," *Plant Ecology and Diversity*, vol. 4, pp. 79–89, 2011.
- [20] J. A. dos Santos, P.-H. Gosselin, S. Philipp-Foliguet, R. da S. Torres, and A. X. Falcão, "Multi-scale classification of remote sensing images," *IEEE Transactions on Geoscience and Remote Sensing*, 2012.
- [21] R. E. Schapire, "A brief introduction to boosting," in *International Joint Conference on Artificial Intelligence (IJCAI'99)*, T. Dean, Ed., 1999, pp. 1401–1406.
- [22] L. Guigues, J. Cocquerez, and H. Le Men, "Scale-sets image analysis," *International Journal of Computer Vision*, vol. 68, pp. 289–317, 2006.